Supplementary material

Electron regulation in Pt-M (M = Cu, Co, and Ni) decorated WO_3 thin films for photocatalytic degradation performance

Jinkang Pan[a,b], Lihua Zhang[b,c], Cunxia Wang[b,c], Kangjie Gao[b,c], and Pengyu Dong[b,*]

[a]School of Chemistry and Chemical Engineering, Yancheng Institute of Technology, Yancheng 224051, P. R. China.

[b]Key Laboratory for Advanced Technology in Environmental Protection of Jiangsu Province, Key Laboratory for Ecological-Environment Materials of Jiangsu Province, Yancheng Institute of Technology, Yancheng 224051, P. R. China.

[c]School of Mechanical Engineering, Yancheng Institute of Technology, Yancheng 224051, People's Republic of China.

* Corresponding author.

E-mail address: dongpy11@gmail.com; dongpy11@ycit.edu.cn (P. Dong)

1. Synthesis of polymethylmethacrylate (PMMA) spheres

An aqueous suspension of monodispersed PMMA microspheres (Ø = 450 ± 5 nm) was synthesized according to the Schroden standard technique [1]. The size of the PMMA spheres produced using this method is highly dependent on the composition of the synthesis mixture and the reaction temperature. Briefly, MilliQ water (400 mL) and methyl methacrylate (MMA, 100 mL) were charged into a 4-necked round-bottomed flask (500 mL in volume), equipped with a mechanical stirrer(glass shaft with Teflon stirrer blade), water-cooled reflux condenser, nitrogen bubbler, and a glass quick-fit stopper. The mixture was then heated to 70 °C, whereupon 2,20-azobis (2-methylpropionamidine) dihydrochloride (0.375 g) was added as an azo-initiator and the polymerization of the MMA started. The reaction mixture was maintained at 70 °C for 2 h under vigorous mechanical stirring and then cooled to room temperature over 3–4 h under a nitrogen purge. The resulting colloidal suspensions of PMMA spheres was finally filtered through a glass wool plug to remove large agglomerates and stored in PET bottles for later use.

2. Supplementary Figures and Table

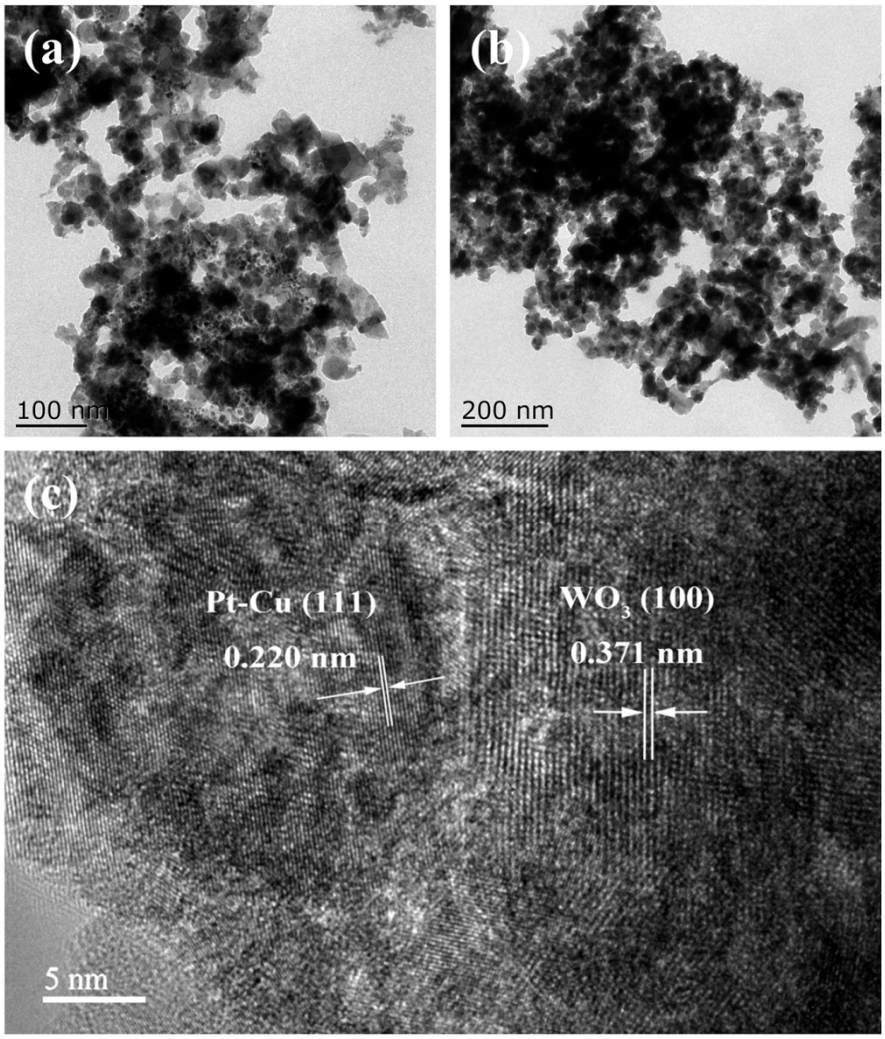

Figure S1. (**a**, **b**) TEM and (**c**) HRTEM images of Pt-Cu/WO_3 thin film.

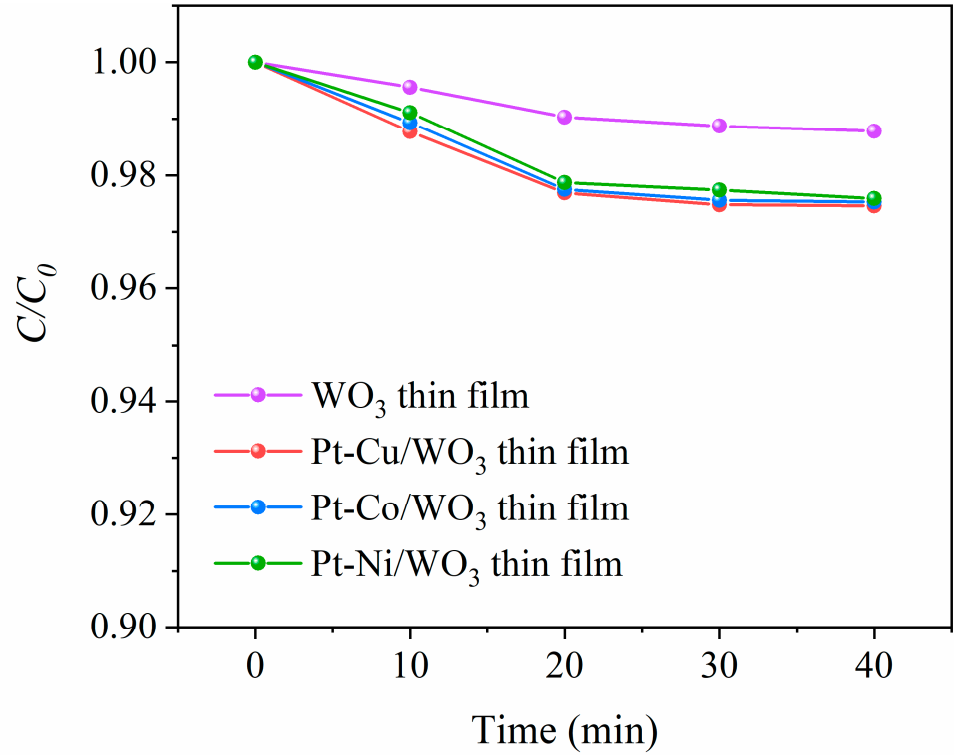

Figure S2. The adsorption isotherms of MB in the presence of as-prepared samples under dark conditions.

Table S1. Comparison between this research and some commonly used WO_3-based photocatalysts for the removal of organic pollutants.

Photocatalyst	Pollutants/Reaction conditions	Degradation efficiency	Rate constant (min^{-1})	Ref.
WO_3	Methylene blue (MB), C_0 = 5 mg L^{-1},100 mL, 120 min. Light source: 300 W Xe lamp, 420 nm cut-off filter.	60 %	0.007	This work
Pt-Cu/WO_3	MB, C_0 = 5 mg L^{-1}, 100 mL, 120 min. Light source: 300 W Xe lamp, 420 nm cut-off filter.	98.9 %	0.040	This work
Pt-Co/WO_3	MB, C_0 = 5 mg L^{-1}, 100 mL, 120 min. Light source: 300 W Xe lamp, 420 nm cut-off filter.	88 %	0.018	This work
Pt-Ni/WO_3	MB, C_0 = 5 mg L^{-1}, 100 mL, 120 min. Light source: 300 W Xe lamp, 420 nm cut-off filter.	90 %	0.019	This work
$FeWO_4$/WO_3	MB, C_0 = 10 mg L^{-1}, 2 h. Light source: 300 W Xe lamp, 420 nm cut-off filter.	90 %	0.0165	[2]
WO_3-rGO	MB, C_0 = 10 mg L^{-1}, 15 mL, 180 min. Light source: 300 W Xe lamp, 420 nm cut-off filter.	78 %	0.008	[3]
WO_3-CuS	MB, C_0 = 5 mg L^{-1}, 250 mL, 60 min. Light source: 300 W Xe lamp, UV cut-off filter.	~ 90 %	0.0288	[4]
WO_3/SiO_2	MB, C_0 = 5 mg L^{-1}, 120 min, pH 7.5. Light source: 65 W Xe lamp, $\lambda > 420$ nm, 125 W/m^2.	91 %	0.013	[5]
WO_3/g-C_3N_4	MB, C_0 = 5 mg L^{-1}, 10 mL, 210 min. Light source: 65 W Xe lamp, 125 W/m^2.	97.82 %	0.0419	[6]
Ag-WO_3	MB, C_0 = 10 mg L^{-1}, 50 mL, 50 min. Light source: 300 W Xe lamp.	88 %	–	[7]
In_2O_3/WO_3	MB, C_0 = 5 mg L^{-1}, 50 mL, 90 min. Light source: 500 W Xe lamp, 420 nm cut-off filter.	92.4 %	0.029	[8]
TiO_2-WO_3	MB, C_0 = 10 mg L^{-1}, 50 mL, 60 min. Light source: 500 W tungsten halogen lamp.	69.8 %	0.0195	[9]

References

1. Rick C. Schroden, M.A.-D., Christopher F. Blanford, and Andreas Stein. Optical properties of inverse opal photonic crystals. *Chem. Mater.* **2002**, *14*, 3305–3315.
2. Liu, C.; Lü, H.; Yu, C.; Ding, B.; Ye, R.; Ji, Y.; Dai, B.; Liu, W. Novel $FeWO_4/WO_3$ nanoplate with p–n heterostructure and its enhanced mechanism for organic pollutants removal under visible-light illumination. *J. Environ. Chem. Eng.* **2020**, *8*, 104044, doi:10.1016/j.jece.2020.104044.
3. Ibrahim, Y.O.; Gondal, M.A.; Alaswad, A.; Moqbel, R.A.; Hassan, M.; Cevik, E.; Qahtan, T.F.; Dastageer, M.A.; Bozkurt, A. Laser-induced anchoring of WO_3 nanoparticles on reduced graphene oxide sheets for photocatalytic water decontamination and energy storage. *Ceram. Int.* **2020**, *46*, 444–451, doi:10.1016/j.ceramint.2019.08.281.
4. Liu, Y.; Li, M.; Zhang, Q.; Qin, P.; Wang, X.; He, G.; Li, L. One-step synthesis of a WO_3-CuS nanosheet heterojunction with enhanced photocatalytic performance for methylene blue degradation and Cr(VI) reduction. *J. Chem. Technol. Biotechnol.* **2019**, *95*, 665–674, doi:10.1002/jctb.6247.
5. Sharma, S.; Basu, S. Highly reusable visible light active hierarchical porous WO_3/SiO_2 monolith in centimeter length scale for enhanced photocatalytic degradation of toxic pollutants. *Sep. Purif. Technol.* **2020**, *231*, 115916, doi:10.1016/j.seppur.2019.115916.
6. Singh, J.; Arora, A.; Basu, S. Synthesis of coral like WO_3/g-C_3N_4 nanocomposites for the removal of hazardous dyes under visible light. *J. Alloys Compd.* **2019**, *808*, 151734, doi:10.1016/j.jallcom.2019.151734.
7. Zhang, J.; Fu, X.; Hao, H.; Gan, W. Facile synthesis 3D flower-like Ag@WO_3 nanostructures and applications in solar-light photocatalysis. *J. Alloys Compd.* **2018**, *757*, 134–141, doi:10.1016/j.jallcom.2018.05.068.
8. Xie, R.; Fang, K.; Liu, Y.; Chen, W.; Fan, J.; Wang, X.; Ren, Y.; Song, Y. Z-scheme In_2O_3/WO_3 heterogeneous photocatalysts with enhanced visible-light-driven photocatalytic activity toward degradation of organic dyes. *J. Mater. Sci.* **2020**, *55*, 11919–11937, doi:10.1007/s10853-020-04863-5.
9. Prabhu, S.; Cindrella, L.; Kwon, O.J.; Mohanraju, K. Photoelectrochemical and photocatalytic activity of TiO_2-WO_3 heterostructures boosted by mutual interaction. *Mater. Sci. Semicond. Process.* **2018**, *88*, 10–19, doi:10.1016/j.mssp.2018.07.028.